Heat-capacity analysis of a large number of $A15$-type compounds

A. Junod, T. Jarlborg, and J. Muller
Département de Physique de la Matière Condensée, Université de Genève, CH-1211 Genève 4, Switzerland
(Received 13 May 1982)

We analyze the low- and medium-temperature specific heat of 25 samples based on eleven $A15$ binary compounds, with T_c's ranging from less than 0.015 to 18 K. Experimentally determined "moments" of the phonon spectra ($\bar{\omega}, \bar{\omega}_2, \omega_{\log}$) are included in the analysis. Values are tabulated for $\bar{T}_c$, $\bar{\alpha}^2$, η, $\langle I^2 \rangle$, $N_{bs}(E_F)$, $M\bar{\omega}_2^2$, $H_c(0)$, and $2\Delta(0)/k_B T_c$. We note the following: (i) The Debye temperature is generally a bad estimate of $\omega_{\log}$. (ii) λ is governed mainly by the "electronic parameter" η; $\lambda = 0.175\eta(\text{eV}/\text{Å}^2) \pm 0.2$ for all $A15$ compounds studied. (iii) η is proportional to the density of states at the Fermi level and this density of states agrees well with band-structure calculations of Jarlborg in Nb-based compounds. In V-based compounds, the observed bad correlation may reflect the presence of spin fluctuations. (iv) The values for the reduced gap $2\Delta(0)/k_B T_c$ range from 3.4 to 4.9 and they are correlated with $T_c/\omega_{\log}$.

I. INTRODUCTION

The measurement of the specific heat of superconductors yields most valuable information provided that a sufficiently wide range of temperature is covered. Typically, this range should extend from about one-tenth of the critical temperature T_c to one-sixth of the Debye temperature. The complete analysis of all data then allows the determination, over and above the electronic specific-heat coefficient and the (initial) Debye temperature $\Theta_D(T=0)$, of a number of characteristic functions. The latter include the formal variation $\Theta_D(T)$, a rough shape of the phonon spectrum $F(\omega)$, the distribution of T_c within somewhat inhomogeneous samples, the thermodynamical critical field $H_c(T)$ and the energy gap $\Delta(0)$ at $T=0$. Further, one may evaluate most of the parameters entering the expression of T_c of Allen and Dynes,[1] i.e., the generalized moments of the phonon spectrum $\omega_{\log}, \bar{\omega}_1, \bar{\omega}_2$, the electron-phonon coupling parameter λ, the bare electronic density of states at the Fermi level N_{bs} (E_F), etc.

In this paper we systematically use a set of programs devised to accomplish the complete analysis of specific-heat data. In view of the importance of the $A15$-type compounds,[2] we shall concentrate on this class of superconductors. The raw data have been previously obtained in our laboratory but only the measurements extending over a sufficiently wide temperature range were retained for the present purpose. The comparative study is, therefore, not complete but the sampling may be considered largely representative: a set of transition temperatures T_c from less than 0.015 to 18.2 K with electronic specific-heat coefficients γ and initial Debye temperatures $\Theta_D(0)$ varying from 2 to 24 $\text{mJ K}^{-2}\text{g-at.}^{-1}$ and 200 to 450 K, respectively. Taking into account the results from alloys with distinct thermal history (ordering), a total of 25 cases will be presented. The following analysis specifically aims at the parameters governing superconductivity, whereas a study of the correlations between the electronic density of states and the form of the phonon spectrum has been published elsewhere.[3]

II. EXPERIMENTAL: SPECIMENS AND CALORIMETRY

The composition of the samples will be labeled V_3Au, Nb_3Au, etc., in spite of the fact that in certain cases, slight deviations from ideal stoichiometry are required to stabilize the $A15$ phase (e.g., $V_{76}Au_{24}$). The reader is referred to a recent review[2] for a comprehensive summary of all known stability limits. Most of the specimens used in this paper have been characterized previously.[3] Three samples of V_3Si are also included here, although the analysis of their specific heat is more delicate as a consequence of the low-temperature martensitic transformation. V_3Si I is a single crystal of mass 3.6 g, its martensitic transition being distributed between 22 and 18.5 K according to the spread of the calorimetric anomaly. V_3Si II is a single crystal of mass 0.46 g with a residual resistance ratio greater than 40. Its anomaly at the martensitic transition is very well defined with a peak of the specific heat at

21.2 K and the onset at 22.2.[4] Finally, V_3Si III is a 20-g polycrystal exhibiting a progressive and probably only partial tetragonal transformation.[5] In the following tables, we distinguish for V_3Si the extrapolations appropriate to the cubic phase ($T > T_m$) from those appropriate to the tetragonal phase ($T_c < T < T_m$). In the latter case, the limited temperature interval gives rise to a more pronounced uncertainty of the extrapolated parameters.

The calorimeter arrangement used for all measurements was of the mechanical-heat-switch type implying quasiadiabatic conditions for the sample plus a heater plus a thermometer system. The accuracy is of the order of 1%. All measurements used here were performed in zero magnetic field.

III. NUMERICAL ANALYSIS

The method of analysis of measured specific-heat curves, equivalent to a simplified inversion, has been described elsewhere.[3] The program worked out for this purpose takes into account the values measured at $T \ll T_c$ which fix the initial Debye temperature, the entropy at T_c (identical to the one measured in

TABLE I. Electron and phonon parameters defining the normal-state heat capacity of the A15-type samples investigated.

	γ $\left[\frac{\text{mJ}}{\text{K}^2\,\text{g-at.}}\right]$	D_1 (%)	T_1 (K)	D_2 (%)	T_2 (K)	D_3 (%)	T_3 (K)	Identification
Nb_3Ir	2.05	−12.6	127	14.6	150	98.0	300[a]	F619C
$Nb_3Pt_{0.6}Ir_{0.4}$	3.92	−1.90	84.0	24.2	207	77.7	300[a]	F912
Nb_3Pt I	5.32	−1.90	70.2	23.6	163	78.4	306	F115
Nb_3Pt II (quenched)	5.74	−1.15	59.4	25.3	175	75.9	307	F911
Nb_3Pt II (annealed)	6.17	−2.22	69.4	17.2	145	85.1	292	F911R
$Nb_3Pt_{0.6}Au_{0.4}$ (quenched)	7.48	−0.859	55.3	20.4	158	80.5	296	F728
$Nb_3Pt_{0.6}Au_{0.4}$ (annealed)	8.38	−1.01	56.0	17.5	145	83.5	300[a]	F728R
$Nb_3Au_{0.7}Pt_{0.3}$ (quenched)	8.40	−0.246	36.9	17.8	151	82.5	293	F727
$Nb_3Au_{0.7}Pt_{0.3}$ (annealed)	10.14	−0.144	31.8	16.3	144	83.8	300[a]	F727R
Nb_3Au	8.96	−0.223	43.2	13.1	135	87.1	284	F726
Nb_3Al	8.72	−0.939	95.1	44.9	220	56.1	400[a]	229R
Nb_3Sn I	14.3	0.025	24.6	13.0	159	87.0	305	B
Nb_3Sn II	12.2	0.814	71.4	26.0	194	73.2	322	K95
$Nb_{78}Sn_{22}$	4.85	−1.92	97.1	5.22	151	96.7	307	ST339
V_3Ir	1.94	−4.14	126	15.9	201	88.3	415	172cs
V_3Pt	7.09	−3.57	103	16.0	173	87.6	374	F500C
V_3Au I (quenched)	8.00	−1.06	72.8	19.4	170	81.6	396	J80T
V_3Au I (annealed)	11.61	−0.828	67.7	20.0	172	80.8	393	J80R
V_3Au II (annealed)	13.09	−1.01	70.9	18.5	164	82.5	389	F161RRR
V_3Au III (A2 phase)	5.02	−0.503	56.2	12.9	139	87.6	367	F1560
V_3Si I ($T < T_m$)	13.2	0.574	60.4	0		99.4	436	ST
V_3Si I ($T > T_m$)	14.7	0.852	60.3	−5.24	145	104.4	400	ST
V_3Si II ($T < T_m$)	14.3	0.282	51.2	0		99.7	405	3-SE
V_3Si II ($T > T_m$)	17.2	0.321	46.3	−3.82	148	103.5	407	3-SE
V_3Si III ($T < T_m$)	13.0	1.09	62.0	−4.49	134	103.4	400[a]	SP
V_3Si III ($T > T_m$)	14.0	0.688	53.2	−3.39	123	102.7	403	SP
V_3Ga (quenched)	19.88	0		4.91	148	95.1	372	237CS
V_3Ga (annealed)	24.22	0.0046	23.3	5.28	149	94.7	372	237CSR
$Ti_3Ir_{0.8}Pt_{0.2}$	8.93	1.63	61.9	0		98.4	291	J210

[a] This parameter could not be defined by the fitting procedure and was arbitrarily set to an average value.

the superconducting state), and all measured specific-heat points between T_c and the upper limit generally set at about 40 K. After adjustment of 4 to 6 parameters, the program yields the electronic specific-heat coefficient γ and a superposition of two to three Debye spectra normalized to $3N$ modes. These parameters, in turn, define the specific heat in the normal state $C_n(T)$, with a variance as low as 0.5% on the average. They are only weakly correlated and reproducible if the results of several independent measurements are used as input data. This would not necessarily be the case for the coefficients of the higher-order terms in a polynomial development of the specific heat containing odd powers of temperature. Another advantage in comparison to the polynomial method is the essential correctness of the high-temperature extrapolation, at least if anharmonic terms are neglected. Further, no preliminary hypothesis is made with respect to the distribution of the number of modes among the different parts of the phonon spectrum.

Table I summarizes the results of the above analysis. The parameters correspond to the formula

$$C_n(T)=\gamma T+\sum_{i=1}^{3} D_i C_D\left[\frac{T}{T_i}\right]\equiv\gamma T+C_{\rm ph}(T)\ , \tag{1}$$

where $C_D(T/\Theta_D)$ is the Debye specific-heat function. At this point one may ask if the low-temperature specific heat contains enough information for the reconstruction of a rough shape of the phonon spectrum $F(\omega)$. Let us demonstrate that this is the case by using a graphic representation introduced by Chambers.[6] It can be shown that certain functionals of the phonon specific heat take the form of convolutions of the phonon spectrum. Particularly, $5/4R\pi^4 C_{\rm ph}T^{-3}$ is an image of the spectrum $\omega^{-2}F(\omega)$ for $\omega=4.928T$, where ω is expressed in degrees kelvin. The response of $C_{\rm ph}T^{-3}$ to a δ function (Einstein peak) is bell-shaped on a logarithmic scale, with a halfwidth of about 0.56.

Consider now a typical experimental result (Figs. 1 and 2, $Nb_3Au_{0.7}Pt_{0.3}$ in the as-cast state) after adjustment of the electronic and phonon parameters in the representation just mentioned (Fig. 3). At the lowest temperatures $T\ll T_c$, the experimental points yield directly $C_{\rm ph}$ because the electronic contribution vanishes exponentially. Above T_c, the term γT is subtracted. The adjusted lattice specific heat is given by the continuous curve. The interpolation in region II is fixed mainly by the condition of equal entropies $S_n=S_s$, whereas the extrapolation in region IV rests on the normalization of the spectrum (equivalent to $C_{\rm ph}\to 3R$). The full curve is the "response" of the specific heat to the parametrized spectrum shown by the dashed line. The logarithmic frequency abscissa is shifted by ln(4.928), the latter number being the solution of $x=5\tanh(x/2)$. The graph of this figure illustrates both the consistency and the limitation of the inversion pro-

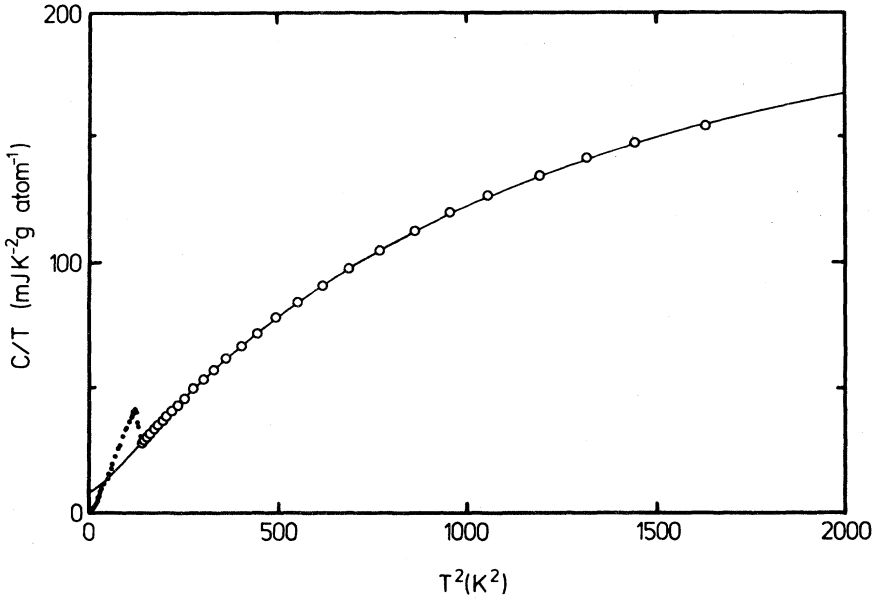

FIG. 1. C/T-vs-T^2 representation of the measured specific heat (circles) and six-parameter curve (see text) fitted to 0.3% rms. The example shown is $Nb_3Au_{0.7}Pt_{0.3}$ in the quenched state.

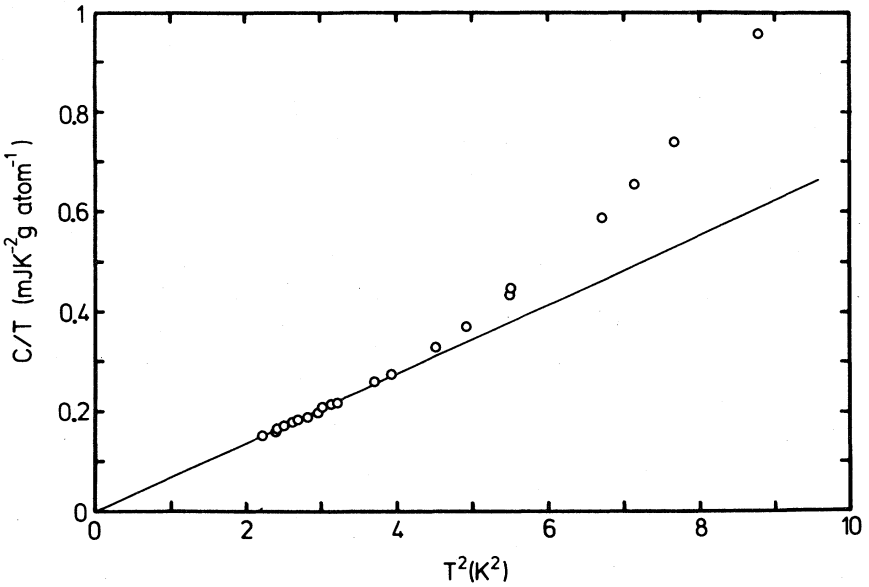

FIG. 2. Expanded data for $T \ll T_c$, example of Fig. 1.

cedure characterizing the phonon spectrum by six quantities D_i and T_i. Other functionals theoretically have a better resolution and respond to higher phonon frequencies but would require an improved experimental accuracy.

For our purpose we do not use directly the model phonon spectra obtained, but use certain of their generalized moments: $\omega_{\log}$, $\bar{\omega}_1$, and $\bar{\omega}_2$. The latter are comparable, with respect to ponderation, to the ordinary moments $\langle \omega^n \rangle$ with $n < 0$: They are determined entirely by the specific heat at low and medium temperatures as demonstrated in a previous publication.[7] The exact form of the model spectrum is, therefore, less important, provided that it is physi-

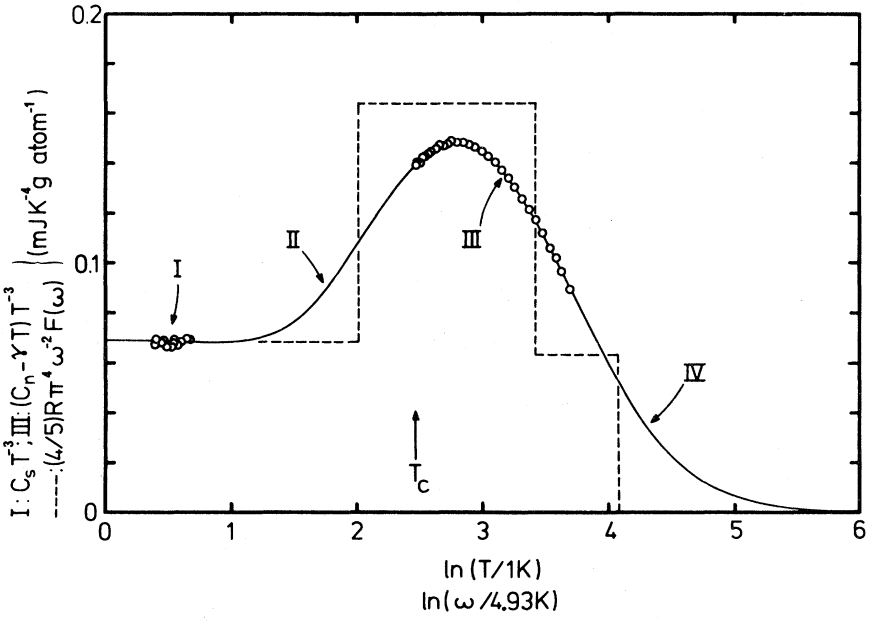

FIG. 3. Dashed step function: Model phonon density of states divided by the frequency squared vs lnω. Continuous curve: Corresponding specific heat divided by T^3 vs ln$T$. Circles: Experimental points, full measured values in region I, γT subtracted in region III for $T > T_c$ ($Nb_3Au_{0.7}Pt_{0.3}$).

cally acceptable and that it allows one to accurately reproduce the observed specific heat. The validity of the above statement may be illustrated by the following comparison in the case of $Nb_3Pt_{0.6}Ir_{0.4}$. With a spectrum given by only two Debye components ($D_1=-1.35\%$, $T_1=77.5$ K, and $D_2=101.35\%$, $T_2=269$ K, root-mean-square deviation 0.85%) one finds $\gamma=3.99$ mJ K^{-2} g-at.$^{-1}$, $\omega_{\log}=155.4$ K, $\bar{\omega}_1=172.4$ K, and $\bar{\omega}_2=183.7$ (see below for the exact definition of these quantities). For the same specimen, the spectrum with three components as given in Table I (rms deviation 0.61%), although different from the first mentioned, yields very similar values $\omega_{\log}=155.0$ K, $\bar{\omega}_1=173.6$ K, and $\bar{\omega}_2=186.8$ K.

For a few samples included in the present study, the parameters γ and $\Theta_D(0)$ differ slightly from those reported previously. This is due to the method of polynomial extrapolation which was used earlier.[8–12] Tests with nonsuperconducting compounds (where the extrapolation procedure may be checked by using a nontruncated set of measurements) have indicated that the present method of analysis is the most reliable one.

With respect to the intrinsic electronic and phonon parameters of homogeneous $A15$ phases, we recall that these quantities not only depend on composition but also on the degree of long-range order. Therefore, for the purpose of data comparison, the specification of thermal treatment is essential.

IV. DETERMINATION OF THE PARAMETERS DESCRIBING SUPERCONDUCTIVITY

In certain polycrystalline specimens, although single phase, inhomogeneities may cause superconducting transitions with an appreciable width. This is the case for Nb_3Pt I (7.9–9.8 K), Nb_3Pt II (7.9–11 K), Nb_3Al (17–18.7 K), and V_3Au I, quenched (0.2–0.8 K). It is then necessary to define a correctly weighted average. For every compound with $T_c>1.2$ K, we have systematically calculated the superconducting volume fraction $f_s(T)$ according to

$$f_s(T)=\frac{C_s-C_n-3(S_s-S_n)}{2\gamma T}, \tag{2}$$

i.e., an expression based on the two-fluid model.[13,14] n and s refer to the normal and superconducting states, S is the entropy, and C is the specific heat. One expects that, for temperatures close to T_c (onset), $f_s(T)$ determined in this way will be slightly underestimated because the specific-heat jump of the two-fluid model is too big in the case of weak coupling. However, the opposite will be true in the case of strong coupling. It is evident that at $T\ll T_c$, $C_s\ll C_n$ ensures the convergence of f_s independently of the model. The definition of $\bar{T}_c$ we use is $f_s(\bar{T}_c)=0.5$. An example is given in Fig. 4, all other results are listed in Table II.

To determine the electron-phonon interaction

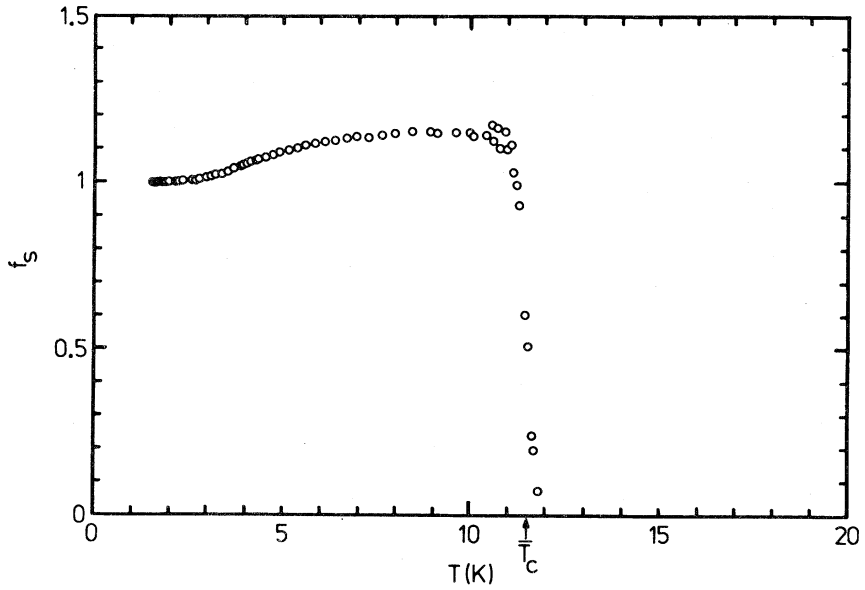

FIG. 4. Superconducting volume fraction $f_s(T)$ to define $\bar{T}_c$ ($Nb_3Au_{0.7}Pt_{0.3}$).

TABLE II. Bulk critical temperature and generalized "moments" of the phonon spectra of A15-type samples.

	$\bar{T}_c$ (K)	$\omega_{\log}$ (K)	$\bar{\omega}_1$ (K)	$\bar{\omega}_2$ (K)
Nb_3Ir	1.48	172	191	203
$Nb_3Pt_{0.6}Ir_{0.4}$	5.73	155	174	187
Nb_3Pt I	8.72	142	161	177
Nb_3Pt II (quenched)	8.81	144	162	177
Nb_3Pt II (annealed)	10.03	141	160	175
$Nb_3Pt_{0.6}Au_{0.4}$ (quenched)	11.45	135	155	171
$Nb_3Pt_{0.6}Au_{0.4}$ (annealed)	12.88	135	156	173
$Nb_3Au_{0.7}Pt_{0.3}$ (quenched)	11.52	128	150	167
$Nb_3Au_{0.7}Pt_{0.3}$ (annealed)	12.85	125	150	169
Nb_3Au	10.59	122	146	164
Nb_3Al	18.07	146	174	196
Nb_3Sn I	17.97	127	157	177
Nb_3Sn II	17.93	123	153	175
$Nb_{78}Sn_{22}$	6.27	160	184	199
V_3Ir	<0.015	204	233	254
V_3Pt	2.73	180	206	225
V_3Au I (quenched)	$0.6+0.2-0.4$	157	188	215
V_3Au I (annealed)	2.15	155	186	212
V_3Au II (annealed)	2.83	154	185	211
V_3Au III (A2 phase)	<0.03	142	175	202
V_3Si I ($T<T_m$)	17.03	183	239	271
V_3Si I ($T>T_m$)		198	247	271
V_3Si II ($T<T_m$)	16.76	184	230	257
V_3Si II ($T>T_m$)		207	253	276
V_3Si III ($T<T_m$)	16.66	190	241	266
V_3Si III ($T>T_m$)		196	246	270
V_3Ga (quenched)	13.56	163	200	226
V_3Ga (annealed)	15.00	161	198	224
$Ti_3Ir_{0.8}Pt_{0.2}$	5.48	119	154	117

parameter λ, we use the expression of Allen and Dynes[1] with $\mu^*=0.13$,

$$T_c=\frac{f_1 f_2 \omega_{\log}}{1.20}\exp\left[-\frac{1.04(1+\lambda)}{\lambda-\mu^*-0.62\lambda\mu^*}\right], \tag{3}$$

where f_1 and f_2 are corrective factors of order unity which depend on the value of λ itself and the shape of the phonon spectrum through $\omega_{\log}$ and $\bar{\omega}_2$. The extraction of λ, therefore, requires a few iterations. The generalized moments $\omega_{\log}$ and $\bar{\omega}_n$ of the electron-phonon spectral function $\alpha^2F(\omega)$ are defined by

$$\ln\omega_{\log}=\frac{\int \alpha^2F(\omega)\ln\omega\, d\ln\omega}{\int \alpha^2F(\omega)\, d\ln\omega}, \tag{4}$$

$$\bar{\omega}_n^{\,n}=\frac{\int \alpha^2F(\omega)\omega^n d\ln\omega}{\int \alpha^2F(\omega)\, d\ln\omega}. \tag{5}$$

The measured specific heat yields information on $F(\omega)$ rather than on $\alpha^2F(\omega)$. One is, therefore, led to introduce an assumption on the form of the function $\alpha^2(\omega)$. Considering that the latter contains only some structure, one may write in first approximation $\alpha^2(\omega)\sim\omega^s$. The exponent s is then "calibrated" by comparing the estimates of $\omega_{\log}$, $\bar{\omega}_1$, and $\bar{\omega}_2$ obtained from the specific heat, for various values of s, with the results of a recent tunneling analysis[15] for Nb_3Sn. The comparison listed in Table III suggests that $s=-\frac{1}{2}$ is the best choice and we shall conserve this type of energy dependence for all other calculations. The spectrum of Nb_3Sn is particularly rich in

TABLE III. Effect of the energy dependence $\alpha^2 \sim \omega^2$ on experimentally determined moments of the phonon spectrum in Nb_3Sn tunneling data from Ref. 15.

Nb_3Sn	s	ω_{log} (K)	$\bar{\omega}_1$ (K)	$\bar{\omega}_2$ (K)
Tunneling		125	152	174
Specific heat	0	155–159	179–181	196–197
	$-\frac{1}{2}$	123–127	153–157	175–177
	-1	81–83	120–123	146–149

low-frequency phonons and one may expect that the effect of the choice of s is less pronounced for the remaining $A15$ compounds. The specific-heat measurements (in the appropriate temperature range) provide us with frequencies $\bar{\omega}_n$ thus defined with an excellent resolution and the results given in Table II allow a coherent description of a variety of compounds.

In order to complete the present computations, we also indicate in Table IV the Debye temperatures

TABLE IV. The Debye temperatures equivalent to the moments of order -3 to $+2$ of the phonon spectra.

	$\Theta_{D,-3}$ (K)	$\Theta_{D,-2}$ (K)	$\Theta_{D,-1}$ (K)	$\Theta_{D,0}$ (K)	$\Theta_{D,1}$ (K)	$\Theta_{D,2}$ (K)
Nb_3Ir	377	323	308	302	300	299
$Nb_3Pt_{0.6}Ir_{0.4}$	347	294	283	281	282	283
Nb_3Pt I	339	274	268	271	277	282
Nb_3Pt II (quenched)	376	277	269	271	276	281
Nb_3Pt II (annealed)	348	272	265	267	271	275
$Nb_3Pt_{0.6}Au_{0.4}$ (quenched)	316	262	260	264	270	275
$Nb_3Pt_{0.6}Au_{0.4}$ (annealed)	320	264	263	269	275	281
$Nb_3Au_{0.7}Pt_{0.3}$ (quenched)	305	253	255	262	268	274
$Nb_3Au_{0.7}Pt_{0.3}$ (annealed)	290	252	258	267	275	281
Nb_3Au	251	244	251	259	265	270
Nb_3Al	292	292	299	310	322	334
Nb_3Sn I	232	259	272	280	286	290
Nb_3Sn II	232	253	268	279	287	293
$Nb_{78}Sn_{22}$	331	309	303	302	303	304
V_3Ir	445	393	386	389	393	397
V_3Pt	403	348	342	346	351	356
V_3Au I (quenched)	342	318	327	342	356	366
V_3Au I (annealed)	338	313	323	338	352	362
V_3Au II (annealed)	332	312	322	338	351	361
V_3Au III (A2 phase)	299	294	310	327	339	347
V_3Si I ($T < T_m$)	297	383	421	431	434	435
V_3Si I ($T > T_m$)	297	396	418	415	410	407
V_3Si II ($T < T_m$)	303	374	397	403	404	405
V_3Si II ($T > T_m$)	303	408	424	420	415	413
V_3Si III ($T < T_m$)	285	384	412	412	408	406
V_3Si III ($T > T_m$)	285	392	417	414	410	408
V_3Ga (quenched)	310	332	347	356	361	365
V_3Ga (annealed)	297	328	344	354	360	364
$Ti_3Ir_{0.8}Pt_{0.2}$	209	251	274	283	287	288

corresponding to the nth moment of the phonon spectrum

$$\Theta_{D,n} \equiv [\tfrac{1}{3}(n+3)\langle \omega^n \rangle]^{1/n} , \tag{6a}$$

$$\Theta_{D,0} \equiv \exp(\tfrac{1}{3} + \langle \ln\omega \rangle) , \tag{6b}$$

where the averages are

$$\langle \omega^n \rangle \equiv \int_0^{\omega\,\max} \omega^n F(\omega) d\omega , \tag{7a}$$

$$\langle \ln\omega \rangle \equiv \int_0^{\omega\,\max} \ln\omega F(\omega) d\omega . \tag{7b}$$

Within this formalism, the Debye temperature of order 2 appears in the high-temperature specific heat,

$$C(T \to \infty) = 3R[1 - (\Theta_{D,2}^2/20T^2)] ,$$

that of order 1 in the zero-point energy, $E_0 = \frac{9}{8} R \Theta_{D,1}$, that of order 0 in the high-temperature lattice entropy,[16]

$$S(T \to \infty) = 4R[1 - \tfrac{3}{4} \ln(\Theta_{D,0}/T)] ,$$

and finally, the limit $n = -3$ leads to the initial Debye temperature $\Theta_D(T \to 0) = \Theta_{D,-3}$.

If the lattice specific heats were governed by the classical Debye model, the temperatures $\Theta_{D,n}$ should be independent of n. Table IV illustrates that this is far from being the case for the compounds investigated. One encounters both the situation $\Theta_{D,-3} > \Theta_{D,2}$ (e.g., Nb_3Ir) as well as $\Theta_{D,-3} < \Theta_{D,2}$ (e.g., Nb_3Sn, $Ti_3Ir_{0.8}Pt_{0.2}$). The differences may be as high as 100 K, a fact which justifies *a posteriori* the relatively complex method of analysis adopted in this paper. Some particularities of the phonon spectra of $A15$ compounds have been discussed in a previous publication.[3]

The unrenormalized electronic density of states at the Fermi level is calculated according to

$$N_{bs}(E_F) = \frac{3\gamma}{2\pi^2 k_B^2 N(1+\lambda)} , \tag{8}$$

where k_B is Boltzmann's constant and N is Avogadro's number. The effect of possible corrections due to spin fluctuations will be discussed later. Further, the present analysis is based on the simplifying assumption of a constant γ up to the limit of the measurements, i.e., 40–45 K. This approximation might be a source of error in the case of V_3Si.

The average $\bar{\alpha}^2$ of the function $\alpha^2(\omega)$, Hopfield's electronic parameter η, and the average $\langle I^2 \rangle$ of the electron-phonon matrix elements are obtained from the expressions

$$\bar{\alpha}^2 = \tfrac{1}{2} \lambda \bar{\omega}_1 , \tag{9}$$

$$\eta = \lambda \bar{M} \bar{\omega}_2^2 , \tag{10}$$

$$\langle I^2 \rangle = \eta / N_{bs}(E_F) , \tag{11}$$

$\bar{M}$ being the mean atomic mass. Following the conclusions of Klein *et al.*[17] we suppose indeed $\eta \simeq \eta_A \gg \eta_B$, the indices A and B referring to the atoms of the formula A_3B. The data of the expressions (9) to (11) are collected in Table V.

The thermodynamical critical field $H_c(T)$ is obtained by integration from the experimental specific heat in the superconducting state C_s and the extrapolated normal-state specific heat C_n through

$$\tfrac{1}{2} \mu_0 V H_c^2(T) = \int_{T_c}^{T} \int_{T_c}^{T'} \frac{C_s - C_n}{T''} dT'' dT' , \tag{12}$$

with V representing the volume per gram-atom. An example of the application of the above relation is shown in Fig. 5. One may also find $H_c(0)$ with a single integration leading to the condensation energy

$$\tfrac{1}{2} \mu_0 V H_c^2(0) = \int_0^{T_c} (C_s - C_n) dT . \tag{13}$$

The results are included in Table VI.

Turning to the determination of the energy gap $\Delta(0)$, we recall that the most direct method would be based on the specific heat at very low temperatures, where

$$C_{es} \sim t^{-3/2} \exp[-\Delta(0)/k_B T] ,$$

with $t \equiv T/T_c \lesssim 0.2$.[18] However, for the compounds studied here, one has to face the problem of the separation of a very small quantity, C_{es}, from a possibly anomalous phonon contribution. Figure 6 illustrates a relatively favorable case, although we would not claim good accuracy for $\Delta(0)/T_c$ determined in this manner. The intermediate range of temperatures ($T \simeq \frac{1}{2} T_c$) is more readily accessible, but the gap is now temperature dependent and requires a model description. The simplest of these is the α model,[19] where the gap is supposed to be the BCS gap multiplied by a constant factor α. The problem then remains to adequately select the temperature range for fitting α. In the case of the critical-field-deviation function (Fig. 7) the weight is placed mainly at temperatures close to T_c. As a consequence, the latter analysis should be used only with very homogeneous specimens. The same is true *a fortiori* for the specific-heat jump at T_c, the measurement of which usually requires an extrapolation. On the other extreme, the semilogarithmic graphs $\ln(C_{es}/\gamma T_c)$ vs T_c/T favor the lowest temperatures where the experimental error (including the effect of minute traces of a normal phase) is greatest. Further, even if it is often assumed tacitly, there is no proof that proportionality holds between the slope of this graph and the reduced gap, the BCS formula

$$C_{es} = 8.5 \gamma T_c \exp(-1.44 T_c/T) ,$$

TABLE V. Calorimetrically determined parameters of $A15$ compounds.

	$N_{bs}(E_F)$ $\left[\frac{\text{states}}{\text{eV at. spin}}\right]$	λ	$\bar{\alpha}^2$ (K)	η (eV/Å^2)	$\langle I^2\rangle$ (eV^2/Å^2)	$\bar{M}\bar{\omega}_2^2$ (eV/Å^2)
Nb_3Ir	0.29	0.51	49	4.4	15.4	8.61
$Nb_3Pt_{0.6}Ir_{0.4}$	0.47	0.78	68	5.7	12.2	7.32
Nb_3Pt I	0.57	0.98	79	6.5	11.4	6.58
Nb_3Pt II (quenched)	0.61	0.98	80	6.5	10.6	6.62
Nb_3Pt II (annealed)	0.63	1.07	85	6.9	10.8	6.42
$Nb_3Pt_{0.6}Au_{0.4}$ (quenched)	0.72	1.19	92	7.4	10.2	6.16
$Nb_3Pt_{0.6}Au_{0.4}$ (annealed)	0.77	1.30	101	8.2	10.5	6.30
$Nb_3Au_{0.7}Pt_{0.3}$ (quenched)	0.80	1.24	93	7.3	9.2	5.91
$Nb_3Au_{0.7}Pt_{0.3}$ (annealed)	0.91	1.36	102	8.2	9.0	6.01
Nb_3Au	0.86	1.21	88	6.9	8.0	5.70
Nb_3Al	0.72	1.59	138	8.3	11.6	5.23
Nb_3Sn I	1.09	1.78	139	9.8	9.0	5.52
Nb_3Sn II	0.92	1.82	140	9.8	10.7	5.38
$Nb_{78}Sn_{22}$	0.57	0.80	73	5.5	9.7	6.95
V_3Ir	0.32–0.41	<0.3	<35	<3	<9	9.91
V_3Pt	0.95	0.59	60	4.6	4.9	7.85
V_3Au I (quenched)	$1.18^{+0.04}_{-0.02}$	$0.44^{+0.03}_{-0.06}$	42^{+2}_{-6}	$3.2^{+0.1}_{-0.5}$	$2.7^{+0.2}_{-0.5}$	7.15
V_3Au I (annealed)	1.57	0.57	53	4.0	2.6	6.96
V_3Au II (annealed)	1.72	0.62	57	4.3	2.5	6.93
V_3Au III (A2 phase)	0.81–1.06	<0.3	<30	<2	<2.5	6.34
V_3Si I ($T<T_m$)	1.24	1.26	151	7.4	6.0	5.90
V_3Si I ($T>T_m$)	(1.42)	(1.20)				5.89
V_3Si II ($T<T_m$)	1.35	1.25	144	6.6	4.9	5.32
V_3Si II ($T>T_m$)	(1.69)	(1.15)				6.10
V_3Si III $T(<T_m)$	1.24	1.22	147	6.9	5.6	5.69
V_3Si III ($T>T_m$)	(1.36)	(1.19)				5.86
V_3Ga (quenched)	1.94	1.17	117	5.9	3.0	5.03
V_3Ga (annealed)	2.27	1.27	126	6.3	2.8	4.96
$Ti_3Ir_{0.8}Pt_{0.2}$	1.02	0.85	66	4.0	3.9	4.66

representing only a numerical interpolation. Following the above considerations, we finally use a normalized plot of $(C_{es}/\gamma T_c)(T/T_c)^{-3}$, in conjunction with a family of curves calculated with the α model. An example is given in Fig. 8, demonstrating that $2\Delta(0)/k_BT_c$ can be determined with a resolution of ± 0.1 to ± 0.2. All other results are listed in Table VI.

To close the present comments on the gap ratio, a further remark on the BCS formula

$$\frac{2\Delta(0)}{k_BT_c}=\frac{4\pi H_c(0)}{T_c}\left[\frac{\mu_0 V}{6\gamma}\right]^{1/2}$$

is in order. The applicability of this relation is frequently misjudged and $\Delta(0)$ may be underestimated in the case of strong coupling. The corrections to $H_c(0)$ and $\Delta(0)$ arising from strong coupling are the following[18]:

$$\frac{H_c(0)}{H_{c\,\mathrm{BCS}}(0)}=\left\{1+2.3\left[\frac{T_c}{\tilde{\omega}}\right]^2\left[\ln\left[\frac{\tilde{\omega}}{T_c}\right]+0.2\right]\right\}^{1/2},$$

$$\frac{\Delta(0)}{\Delta_{\mathrm{BCS}}(0)}=1+5.3\left[\frac{T_c}{\tilde{\omega}}\right]^2\ln\left[\frac{\tilde{\omega}}{T_c}\right],$$

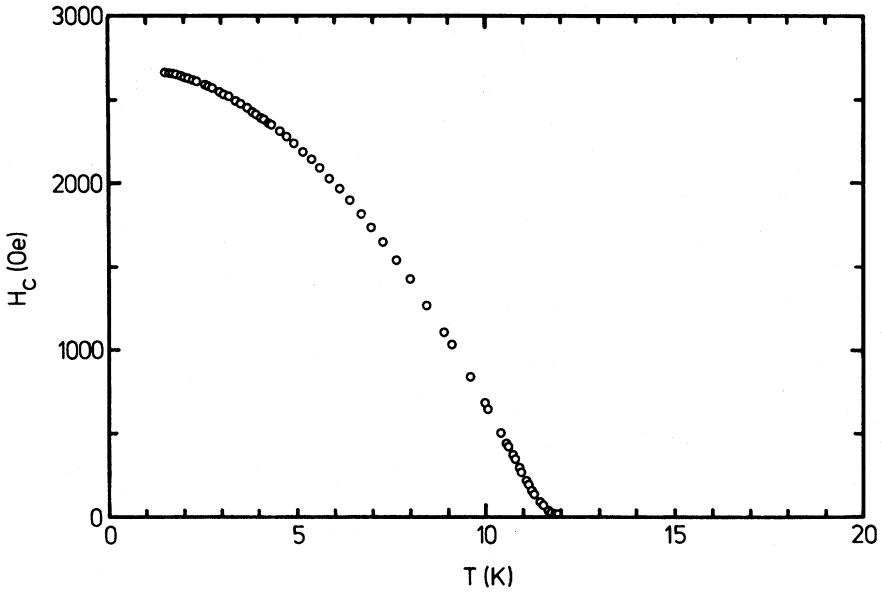

FIG. 5. Thermodynamical critical field H_c vs T ($Nb_3Au_{0.7}Pt_{0.3}$).

where $\tilde{\omega}$ denotes the frequency of the first peak of the phonon density of states. The proportionality between $H_c(0)$ and $\Delta(0)$ is, therefore, not conserved. The same conclusion follows from the α model. The simple use of $H_c(0)$ to estimate $\Delta(0)$ may still be desirable, but such an evaluation should be based on the data tabulated by Padamsee *et al.*[19] rather that the BCS formula.

V. DISCUSSION

A. Preliminary remarks

If the emphasis were on the complete characterization of one particular superconductor, the hypotheses and approximations used so far might be questionable to some extent. For instance, we

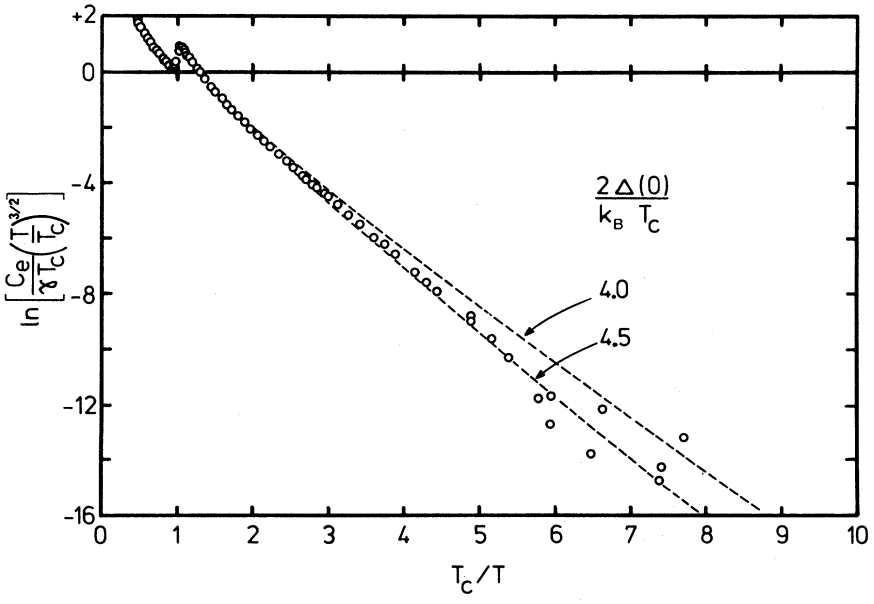

FIG. 6. Semilogarithmic plot of the electronic specific heat. Dashed curves: α model for $2\Delta(0)/k_BT_c=4.0$ and 4.5 ($Nb_3Au_{0.7}Pt_{0.3}$).

TABLE VI. Additional properties of $A15$ compounds.

	$\overline{M}$ $\left[\frac{\text{g}}{\text{g-at.}}\right]$	$\overline{V}$ $\left[\frac{\text{cm}^3}{\text{g-at.}}\right]$	$H_c(0)$ (kOe)	$\frac{2\Delta(0)}{k_B T_c}$	$\frac{T_c}{\bar{\omega}_{\log}}$
Nb_3Ir	117.7	10.18			0.0086
$Nb_3Pt_{0.6}Ir_{0.4}$	118.2	10.26	0.89	3.6	0.037
Nb_3Pt I	118.5	10.31	1.60	3.8	0.061
Nb_3Pt II (quenched)	118.5	10.31	1.67	3.9	0.061
Nb_3Pt II (annealed)	118.5	10.31	1.96	3.9	0.071
$Nb_3Pt_{0.6}Au_{0.4}$ (annealed)	118.6	10.45	2.53	4.3	0.085
$Nb_3Pt_{0.6}Au_{0.4}$ (annealed)	118.6	10.45	3.02	4.4	0.096
$Nb_3Au_{0.7}Pt_{0.3}$ (quenched)	118.8	10.53	2.72	4.3	0.090
$Nb_3Au_{0.7}Pt_{0.3}$ (annealed)	118.8	10.53	3.34	4.4	0.103
Nb_3Au	118.9	10.60	2.57	4.4	0.087
Nb_3Al	76.4	10.47	4.33	4.5	0.125
Nb_3Sn I	99.4	11.13	5.36	4.8	0.14
Nb_3Sn II	99.4	11.13	5.06	4.9	0.145
$Nb_{78}Sn_{22}$	98.6	11.03	1.05	3.6	0.004
V_3Ir	86.3	8.26			
V_3Pt	87.0	8.41	0.63	3.4	0.015
V_3Au I (quenched)	87.5	8.75			0.004
V_3Au I (annealed)	87.5	8.75	0.58	3.4	0.014
V_3Au II (annealed)	87.5	8.75	0.87	3.5	0.018
V_3Au III (A2 phase)	87.5	8.65			
V_3Si I ($T<T_m$)	45.2	7.95	5.72	4.1	0.093
	45.2	7.95	5.78	4.0	0.091
	45.2	7.95	5.52	4.0	0.088
V_3Ga (quenched)	55.6	8.44	5.58	4.6	0.083
V_3Ga (annealed)	55.6	8.44	6.71	4.5	0.0935
$Ti_3Ir_{0.8}Pt_{0.2}$	84.1	9.48	1.35	3.8	0.046

neglect the fact that the cutoff of the electron-phonon interaction at higher energies may reflect not only the phonon spectrum but also the electronic density of states.[20] Furthermore, we implicitly reduce the properties of a compound to those mainly of an atomic nature, described by average parameters λ, η, etc. However, our aim is clearly to evaluate a large number of physical parameters in a most systematic way. The results will show, contrary to previous rather inconclusive statements, that correlations do exist between superconducting properties and *average* phonon and electronic properties. The consideration of a sufficient number of substances is essential in this respect.

B. Thermodynamical critical field and energy gap

The highest thermodynamical critical field is observed in V_3Ga, amounting to 6.7 kOe at $T=0$. This maximum value is related to the high electronic density of states which is also extreme within the $A15$ class. Despite its higher T_c, Nb_3Sn ranks second with 5.2 kOe. The deviations of $H_c(T)$ from the parabolic law (Fig. 7) are confined within the limits of the BCS prediction and the curve for elementary lead. Taking into account the comments already made in Sec. IV, these deviations scale with the reduced gap parameters $2\Delta(0)/k_B T_c$ of Table

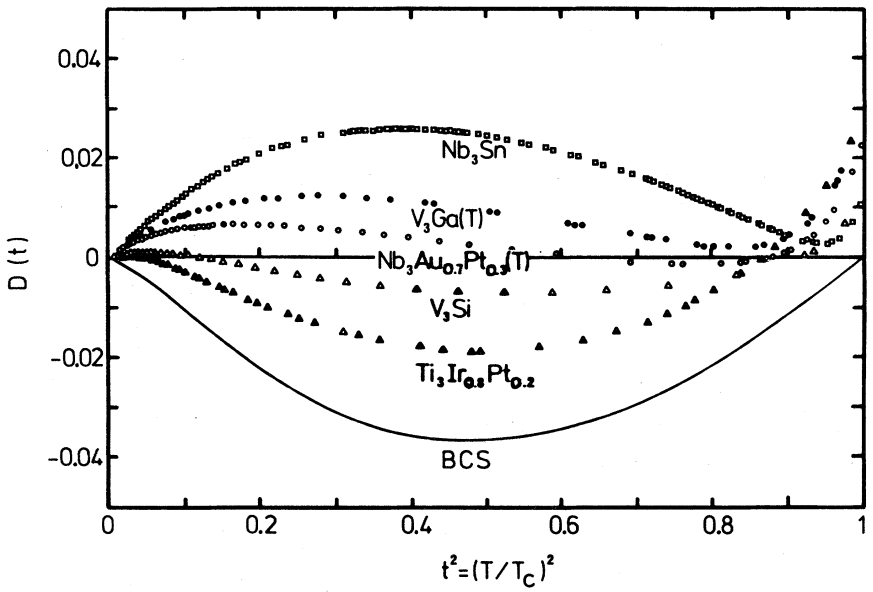

FIG. 7. Deviation function $[H_c(T)/H_c(0)]-[1-(T/T_c)^2]$ vs $(T/T_c)^2$.

VI. While the lowest values of the latter set do not fall significantly below the BCS limit, the numbers correlate with the coupling strength expressed as the ratio of T_c and a typical phonon frequency. A comparison of Nb_3Sn and nonstoichiometric $Nb_{0.78}Sn_{0.22}$ is particularly indicative: The former, with a high T_c and an appreciable density of long-wavelength phonons, exhibits a maximum of 4.8 to 4.9 for $2\Delta(0)/k_BT_c$, whereas the latter, markedly stiffer and with lower T_c, yields the weak coupling figure of 3.6. In order to visualize this correlation, we report in Fig. 9 the gap ratio as a function of $T_c/\omega_{\log}$. The behavior predicted by the model of Geilikman and Kresin,[21] i.e.,

$$\frac{2\Delta(0)}{k_BT_c}=3.53\left[1+5.3\left[\frac{T_c}{\tilde{\omega}}\right]^2\ln\left[\frac{\tilde{\omega}}{T_c}\right]\right], \quad (14)$$

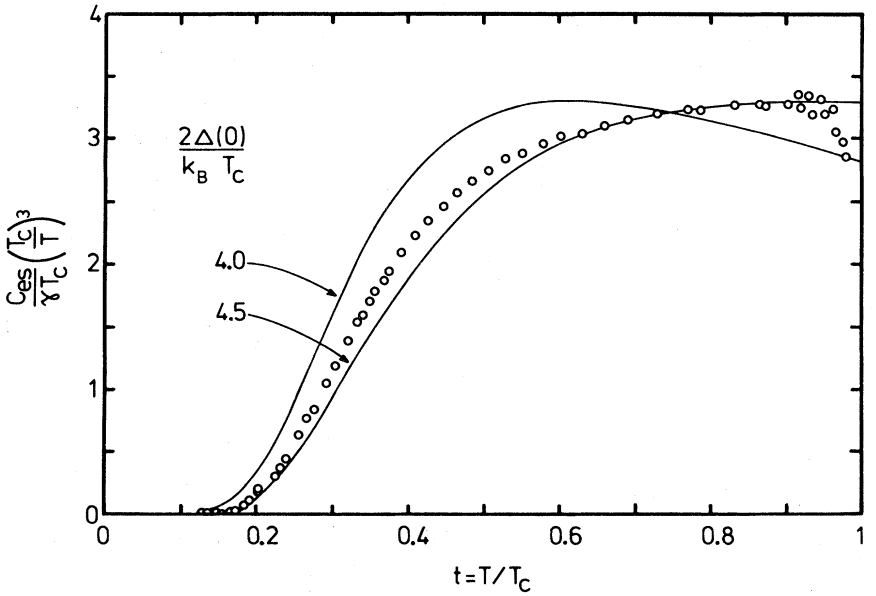

FIG. 8. Electronic specific heat below T_c divided by T^3 vs T/T_c. Solid curves: α model for $2\Delta(0)/k_BT_c=4.0$ and 4.5 ($Nb_3Au_{0.7}Pt_{0.3}$).

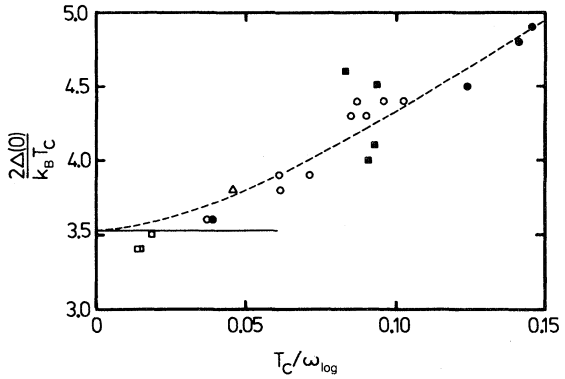

FIG. 9. Reduced energy gap vs T_c/ω_{log}. ○, Nb_3X; □, V_3X; △, Ti_3X; Horizontal line, BCS value. Dashed curve, model of Geilikman and Kresin with $\tilde{\omega}=\frac{2}{3}\omega_{log}$.

is indeed observed if $\tilde{\omega}$ is identified roughly with $\frac{2}{3}\omega_{log}$.

C. Comparison of $\Theta_D(0)$ and ω_{log}

Allen and Dynes[1] have shown that the characteristic phonon frequency entering as a prefactor in the McMillan formula is ω_{log}. Since this quantity is only known for a few $A15$ compounds, it is customary to replace it by a certain fraction of the Debye temperature. Tables II and IV, however, demonstrate that $\Theta_D(0)$ is not a good substitute for ω_{log}. In the case of $Nb_3Au_{0.7}Pt_{0.3}$ and V_3Si, the values of $\Theta_D(0)$ are similar but those of ω_{log} differ by 50%. Conversely, the $\Theta_D(0)$ values differ by 150 K for $Ti_3Ir_{0.8}Pt_{0.2}$ and Nb_3Pt, yet their averages ω_{log} are much closer to each other.

As a consequence, at least in the $A15$ class, the determination of λ from calorimetric data requires more information on the phonon spectrum than the mere curvature in the limit $\omega=0$. This requirement implies specific-heat measurements up to temperatures permitting to probe the essential part of the spectrum. To our knowledge, only a single heat-capacity study has been directed beyond the Debye approach in the past. Knapp *et al.*[16] used measurements at high temperatures ($T\gtrsim\Theta$) to obtain the Debye temperature of order zero, $\Theta_{D,0}$ [$\Theta_D(n=0)$ in their notation[16]] which is related to the geometric mean frequency ω_g [$\equiv(\prod_{s=1}^{3N}\omega_s)^{1/3N}$]. Unfortunately, their evaluations of λ are not comparable to ours for two reasons: ω_g gives more weight to high frequencies than does ω_{log}, and the use of the McMillan formula results in a different prefactor. For the example of Nb_3Sn, Knapp *et al.* indicate the exponential factor as $\omega_g/1.45T_c\simeq 10.8$, whereas the present analysis infers $\omega_{log}/1.2T_c\simeq 5.8$, in agreement with tunneling results.

D. Electronic density of states

In Table VII the experimental densities of states deduced from the present specific-heat analyses are compared with the results of recent band-structure calculations (N^c).[17,22–26] In the graph of Fig. 10, only the results of Jarlborg[22] are retained since they cover the greatest number of compounds. The experimental values are completed by estimates based on the following published measurements: Stewart and Webb[27] for Nb_3Ga, Stewart *et al.*[28] for Nb_3Ge, Knapp *et al.*[16] for Nb_3Sb, and Spitzli[5] for V_3Ge,

TABLE VII. Calorimetrically determined bare density of states at the Fermi level, and calculated values according to Refs. 17 and 22–26.

	$N^\gamma(1+\lambda)^{-1}$	N^c (states eV^{-1} at.$^{-1}$ spin^{-1})			
	$\frac{\text{states}}{\text{eV at. spin}}$	Jarlborg	Klein	Pickett	Van Kessel
Nb_3Ir	0.29	0.44			
Nb_3Pt	0.63	0.6–0.8			
Nb_3Au	0.86	1.10			
Nb_3Al	0.72	0.84	0.91	0.97	
Nb_3Sn	0.92–1.09	0.99	0.73		1.12
V_3Ir	0.32–0.41	0.34			
V_3Pt	0.95	0.83			
V_3Au	1.72	1.51			
V_3Si	1.24–1.35	0.80	0.92		
V_3Ga	2.27	1.28	1.23		

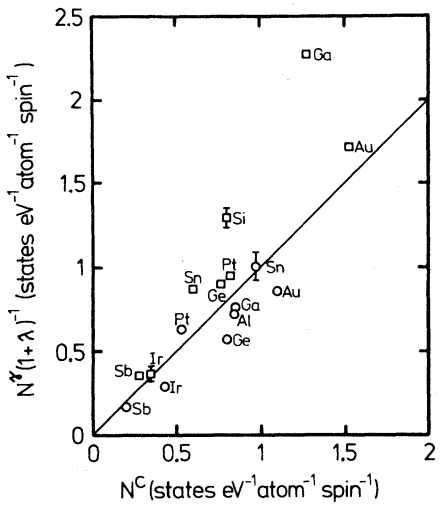

FIG. 10. Empirical electronic density of states at E_F vs calculated value N^c. ○, Nb_3X; □, V_3X.

$V_{\sim 3}Sn$, and V_3Sb. To derive $N^{\gamma}(1+\lambda)^{-1}$ from these measurements, we have estimated $\omega_{\log}$, $\bar{\omega}_1$, and $\bar{\omega}_2$ in relation to $\Theta_D(0)$ (see below for details). It seems satisfactory that an approximate equality $N^{\gamma}(1+\lambda)^{-1} \simeq N^c$ holds for most of the compounds, especially those based on niobium. The uncertainties in the empirical determination of $N^{\gamma}(1+\lambda)^{-1}$ arising from the use of a common value of μ^*, deviations from stoichiometry, partial disorder, the hypothesis on $\alpha^2(\omega)$, on the one hand, and the uncertainties in the band-structure results, on the other hand, may contribute to explain the dispersion. One remarks, however, two notorious exceptions: V_3Si and especially V_3Ga.

In the latter case the source of the disagreement, which amounts to 80%, is not likely to be in the specific-heat analysis. Indeed, the experimental determination of γ by extrapolation encounters no particular risk of error for V_3Ga. It is also unlikely that the empirical method of evaluation of λ, which seems satisfactory for the rest of the compounds, fails dramatically for V_3Si and V_3Ga. If it were so, one would have to conclude that $\alpha^2(\omega)$ decreases much more rapidly than $\omega^{-1/2}$ in these two compounds, implying $\omega_{\log} \simeq 4T_c$ for V_3Ga. As a thermodynamical consequence of such extreme strong coupling,[18] the specific-heat discontinuity at T_c should then be about twice as high as actually observed ($\Delta C/\gamma T_c = 2.2$). A way out of these contradictions is to assume additional renormalizations of the density of states, particularly due to spin fluctuations. Evidence for such effects will be discussed in the last paragraph of this section. In some other systems, the existence of spin fluctuations appeared to be linked with the presence of vanadium atoms $Nb_{1-x}V_x$, (Refs. 30 and 31), and $Nb_{1-x}V_xN$.[32] In Fig. 10 the V-based compounds tend to be *above* the Nb-based compounds, an indication which points to the same conclusion.

E. Effect of partial disorder

In several cases a sizable variation of the calorimetrically measured T_c has been obtained with thermal treatment. The data of the present study enable us to identify the main factors governing these T_c variations (Table VIII). The degree of long-range order does not appreciably influence $\omega_{\log}$, the origin of the T_c increase upon annealing is, therefore, not to be looked for in this quantity. The role of the higher phonon frequencies, influencing λ through the moment $\bar{\omega}_2^2$, is more difficult to assess because of the limited sensitivity of the specific-heat

TABLE VIII. Relative shifts of parameters due to heat treatment or to a change of stoichiometry.

	$\frac{\Delta\lambda}{\lambda}$	$\frac{\Delta N_{bs}(E_F)}{N_{bs}(E_F)}$	$\frac{\Delta\langle I^2\rangle}{\langle I^2\rangle}$	$\frac{\Delta n}{\eta}$	$\frac{\Delta\bar{\omega}_2^2}{\bar{\omega}_2^2}$	$\frac{\Delta\omega_{\log}}{\omega_{\log}}$
Effect of ordering						
Nb_3Pt	+8.6%	+3.1%	+2.3%	+5.4%	−3.0%	−1.8%
$Nb_3Pt_{0.6}Au_{0.4}$	+8.5%	+7.1%	+3.6%	+10.9%	+2.3%[a]	−0.0%
$Nb_3Pt_{0.3}Au_{0.7}$	+9.7%	+14.6%	−2.6%	+11.5%	+1.7%[a]	−2.1%
V_3Au I	+29%	+33%	−6%	+26%	−2.6%	−1.5%
V_3Au I→II	+7.7%	+9.6%	−2.0%	+7.3%	−0.4%	−0.7%
V_3Ga	+8.1%	+16.7%	−8.6%	+6.6%	−1.4%	−1.6%
Effect of stoichiometry						
$Nb_{78}Sn_{22}$ →Nb_3Sn I	+123%	+91%	−7%	+77%	−21%	−21%
$Nb_{78}Sn_{22}$ →Nb_3Sn II	+129%	+60%	+10%	+77%	−23%	−23%

[a]Not significant (see text).

analysis at these frequencies. If one writes (for each particular compound)

$$\frac{\Delta\lambda}{\lambda}=\frac{\Delta N_{bs}(E_F)}{N_{bs}(E_F)}+\frac{\Delta\langle I^2\rangle}{\langle I^2\rangle}-\frac{\Delta\bar{\omega}_2^2}{\bar{\omega}_2^2}\ . \tag{15}$$

Table VIII suggests in general terms:

(i) The variation of the electronic density of states and in most cases that of $\bar{\omega}_2^2$ both contribute positively to the increase of λ. [Note: The apparent exceptions for $\bar{\omega}_2^2$ of $Nb_3Pt_{0.6}Au_{0.4}$ and $Nb_3Pt_{0.3}Au_{0.7}$ may be due to the technical procedure. The specific heat in the annealed state was not measured to sufficiently high temperatures, one parameter of Table I (T_3) was, therefore, fixed arbitrarily near that of the quenched state.]

(ii) The contribution of $\Delta\eta/\eta$ is definitely more important than that of $\Delta\bar{\omega}_2^2/\bar{\omega}_2^2$.

(iii) $\Delta\langle I^2\rangle/\langle I^2\rangle$ which tends to be negative for $\Delta\lambda>0$, compensates only partially the relative change in the density of states.

In summary, the ordering effects observed here mainly influence T_c through the electronic density of states, rather than through a shift of the phonon frequencies. The differences generated by compositional variations in the Nb-Sn system lead to an analogous conclusion although the phonon softening in ideal Nb_3Sn is more pronounced (Table VIII).

F. Correlations between λ, $N_{bs}(E_F)$, $\langle I^2\rangle$, and $\langle\omega^2\rangle$

Can we generalize the conclusions of the preceding paragraph to the relations between properties of different $A15$ compounds? Contradictory points of view have been expressed in the literature[33–35] regarding the predominance of either the "electronic" or the phonon factor in the variations of $\lambda=\eta(M\bar{\omega}_2^2)^{-1}$ among superconducting materials.

In Fig. 11 the plot of λ as a function of the electronic term η reveals a strong correlation between these quantities. This means that, on the whole, $M\bar{\omega}_2^2$ (the "lattice rigidity" or a kind of average force constant) does not deviate too much from an average value. The latter, corresponding to the inverse slope of the figure, is 5.7 eV Å^{-2}. Such a behavior is not unexpected for a given type of bonding. We should like to point out, however, that the product $M\Theta_D^2(0)$ undergoes more important variations because the sound velocity is influenced by the electronic density of states. A "compensation" of the respective variations of $N_{bs}(E_F)$ and $\langle I^2\rangle$, as suggested earlier,[33,34] is not borne out by the data of Fig. 11, but closer inspection allows one to detect the influence of the phonons: The points above the straight line represent compounds with important phonon densities at low frequencies (their effective Debye temperature is monotonically increasing with T), conversely, those below the line exhibit the normal behavior with $\Theta_{D,\mathrm{eff}}(T)$, passing through a minimum. We conclude that the extra contribution to λ arising from the presence of soft phonons amounts to the order of $\Delta\lambda\lesssim 0.3$–$0.4$.

The correlation between λ and η being established, the next question is to find out if there is a clear overall dependence of η on the electronic density of states. The answer depends on the atom placed on the chain site. Figure 12(a) shows η vs $N_{bs}(E_F)$ for niobium-based compounds. The data include estimated values for Nb_3Rh, Nb_3Os,[5] Nb_4Sb, Nb_3Sb,[5,16] Nb_3Ga, and Nb_3Ge.[27,28] For the first four, we set $\omega_{\log}\simeq 0.45\Theta_D(0)$, $\bar{\omega}_1\simeq 0.5\Theta_D(0)$, $\bar{\omega}_2\simeq 0.55\Theta_D(0)$ by analogy with the compounds Nb_3Ir, Nb_3Pt, and Nb_3Au. Nb_3Ga and Nb_3Ge are supposed to be similar to Nb_3Al with $\omega_{\log}\simeq 0.5\Theta_D(0)$, $\bar{\omega}_1\simeq 0.6\Theta_D(0)$, $\bar{\omega}_2\simeq 0.67\Theta_D(0)$. Generally speaking, the distribution of points in Fig. 12(a) suggests a simple proportionality between η and $N_{bs}(E_F)$. An equivalent statement is to admit a roughly common value of $\langle I^2\rangle\simeq 11$ eV/Å^2 characteristic of the Nb atom in the $A15$ structure. Such a rule is in qualitative agreement with the calculations of Klein *et al.*[17] Nb_3Ge still seems to remain an exception, at least in the absence of a more reliable value for $\bar{\omega}_2^2$.

All things considered, the microscopic parameters describing superconductivity of the niobium-based $A15$ compounds follow a rather simple tendency approximately expressed by $\lambda/N_{bs}(E_F)\simeq 1.7$ eV at. spin. This reflects the picture of superconductivity being determined by the sublattice of the Nb atoms, while the B atoms manifest themselves through the lattice constant (i.e., the bandwidth) and electron transfer (i.e., the potential and the Fermi energy), and to a minor extent through a shift of certain phonon frequencies.

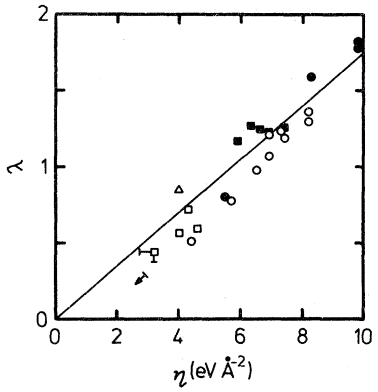

FIG. 11. Electron-phonon interaction parameter λ vs $\eta=\lambda M\bar{\omega}_2^2$. ○, Nb_3X; □, V_3X.

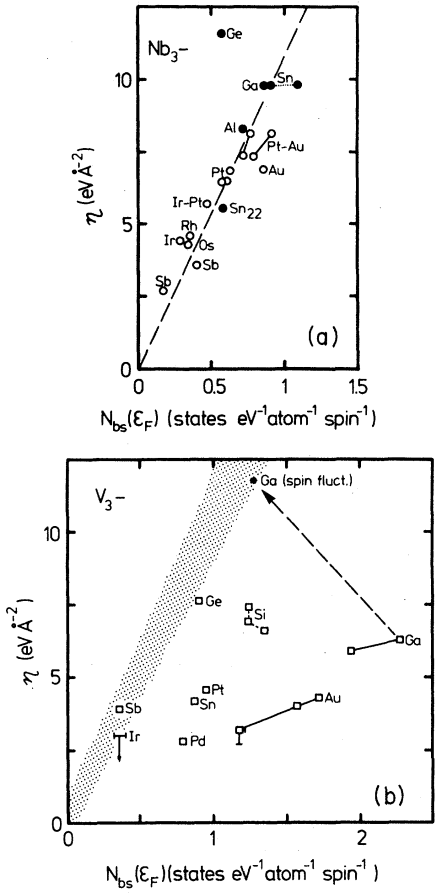

FIG. 12. Electronic parameter η vs empirical density of states $N_{bs}(E_F)$ for Nb_3X compounds. (b) Same plot as (a) for V_3X compounds. Hatched area: Nb_3X.

In the vanadium-based compounds, the situation is unfortunately less clearcut. It would be tempting to derive a second average value of $\langle I^2\rangle$ characteristic of the vanadium atoms in the $A15$ structure. Figure 12(b) shows that this is not possible in the framework of the present formalism. It is true that the different states of order of V_3Ga and V_3Au would define a low mean value of $\langle I^2\rangle \simeq 2.8$ eV/Å^2 but most other compounds are far off. For the four compounds included from earlier work,[5] i.e., V_3Pd, V_3Ge, V_3Sn, and V_3Sb, we used the estimates $\omega_{log}\simeq 0.5\Theta_D(0)$, $\omega_1\simeq 0.6\Theta_D(0)$, and $\bar{\omega}_2\simeq 0.67\Theta_D(0)$, in conformity with the average trends of Tables II and IV. These approximations may introduce uncertainties as high as 40% for the four respective values of η through the term $\bar{\omega}_2^2$.

G. Spin fluctuations?

Suppose that the simple relation between η and $N_{bs}(E_F)$ is hidden by the presence of important spin fluctuations in V_3X compounds. We then ask the question if the consequences of this hypothesis are compatible with the measurements. First, it is remarkable indeed that V_3Ga, which exhibits by far the highest electronic specific heat, does not do better in terms of T_c. Second, we have seen that the empirical density of states is far above that of two independent band-structure calculations. These two facts may be related. Spin fluctuations indeed modify the thermal effective mass via a formal interaction parameter λ_{sf}:

$$N^\gamma = N_{bs}(1+\lambda_{e\text{-ph}}+\lambda_{sf}) , \tag{16}$$

where $N^\gamma = 3\gamma(2\pi^2 k_B^2)^{-1}$ and $\lambda_{e\text{-ph}}$ is the electron-phonon interaction parameter exclusively considered so far. The effect on the superconducting transition temperature is taken into account by replacing λ and μ^* in the expression of Allen and Dynes by effective values,[36,37]

$$\lambda_{eff} = \lambda_{e\text{-ph}}(1+\lambda_{sf})^{-1} , \tag{17}$$

$$\mu^*_{eff} = (\mu^* + \lambda_{sf})(1+\lambda_{sf})^{-1} , \tag{18}$$

which cause a reduction of T_c. Given the quantities N^γ, $N_{bs}=N^c$, and T_c/ω_{log} [under the assumption that $\alpha^2(\omega)\sim\omega^s$ is maintained], $\lambda_{e\text{-ph}}$ and λ_{sf} can be calculated. Inspection of Table VII shows that the results for λ_{sf} will be significant only for V_3Si and V_3Ga. The case of V_3Si is somewhat delicate due to the low martensitic transformation temperature; therefore, we restrict the evaluation to V_3Ga. For the latter, one obtains $\lambda_{eff}=2.17$, $\mu^*_{eff}=0.31$, $\lambda_{e\text{-ph}}=2.75$, $\lambda_{sf}=0.27$, $\eta=13.6$ eV Å^{-2}, and $\langle I^2\rangle = 10.6$ (eV/Å)^2. The new representative point is indicated by a star in Fig. 12(b) and falls approximately in the range of the Nb_3X compounds. It appears that the corrections are important and that they may seriously modify the relation between $\lambda_{e\text{-ph}}$ and $N_{bs}(E_F)$.

Spin fluctuations cause a well-known enhancement of the Pauli magnetic susceptibility χ_P. With the definition of the enhanced density of states $N^\chi = \chi_P/2\mu_B^2$, one relates the Stoner factor $S\equiv N^\chi/N_{bs}$ to λ_{sf} by[38]

$$\lambda_{sf} = 4.5\left[1-\frac{1}{S}\right]\ln\left[1+p_1^2\frac{S-1}{12}\right] , \tag{19}$$

where p_1^2 is an adjustable cutoff parameter. The isolation of a moderate Stoner factor $S\gtrsim 1$ is problematic because in general, the spin susceptibility χ_p cannot be separated unambiguously from the total susceptibility χ. A reasonable assumption, however, is to attribute variations of χ upon increasing the long-range order parameter to χ_P alone, i.e.,

$\Delta\chi=\Delta\chi_P$. The ratio of the small changes of γ and χ due to annealing then yields

$$\frac{\Delta N^{\chi}}{\Delta N^{\gamma}}\simeq\frac{S}{1+\lambda_{e\text{-ph}}+\lambda_{sf}}\ , \tag{20}$$

and experiment finally allows one to determine the parameter p_1 which should be of order unity.[39] Taking for V_3Ga in the two states of order reported here, $\chi=413\times10^{-6}$ and 449×10^{-6} emu/g-at., respectively,[40] one finds $\Delta N^{\chi}/\Delta N^{\gamma}=0.86$, and with the numbers for $\lambda_{e\text{-ph}}$ and λ_{sf} given before, $p_1\simeq0.66$. Leaving aside the ordering experiments but by making use of the orbital susceptibility inferred from NMR,[41] we obtain $N^{\chi}/N^{\gamma}=0.87\pm0.1$ and $p_1\simeq0.65\pm0.06$. For comparison, $p_1\simeq0.6$ in the case of Pd.[39] The order of magnitude is correct.

On first sight, the situation is less readily understood for V_3Au. In this case, the band-structure calculation provides the highest density of states ever computed for an $A15$ compound. The observed T_c of only about 3 K and the ratio $\Delta N^{\chi}/\Delta N^{\gamma}=2.2$, which is higher than for V_3Ga, might be explained by the presence of spin fluctuations. Interesting enough (Table VII), $N^{\gamma}(1+\lambda)^{-1}$ and N^c do not differ much and provide little margin to introduce λ_{sf} for renormalization. We believe that in this case, the band calculations and the experiments do not describe the same physical crystal. We recall that T_c is strongly subject to the degree of order.[42,43] It is, therefore, likely that the alloy with $T_c=2.9$ K [of composition close to $V_{76}Au_{24}$ and with a Bragg-Williams parameter $S_a=0.94\pm0.02$ (Ref. 43)] is still too disordered and has too low a density of states N^{γ} to be compared with the calculated ideal compound. On the other hand, since the Fermi energy is right in a peak of the density of states, a refinement of the band-structure calculations with the use of a nonspherical potential would lead to a lower N^c. These combined effects will certainly allow one to postulate a sizable value of λ_{sf} which depends on N^{γ}/N^c.

VI. CONCLUSION

The detailed analysis of the specific heat of 25 specimens with the $A15$-type structure leads to the following main results:

(i) The initial Debye temperature in the limit $T\to0$ is generally *not* representative of the phonon frequencies important for superconductivity.

(ii) The reduced energy gap $2\Delta(0)/k_BT_c$ takes values between 3.4 and 4.9 and is correlated with $T_c/\omega_{\log}$.

(iii) λ is governed essentially by the electronic parameter η. An average relation $\lambda=0.175\eta$ (eV/Å^2) ±0.2 holds for all compounds studied.

(iv) For the niobium-based compounds, η is proportional to $N_{\text{bs}}(E_F)$, while for vanadium-based compounds, such a simple relation appears to be hidden by the presence of spin fluctuations.

ACKNOWLEDGMENTS

We thank Professor H. Rietschel for having drawn our attention to the likely importance of spin fluctuations in V_3Ga. We also express our gratitude to the members of the metallurgy group of our department for their help with the preparation of specimens. One of us (T.J.) thanks Professor M. Peter for his encouragement to perform the new band-structure calculations. This work has been supported by the Fonds National Suisse de la Recherche Scientifique.

[1]P. B. Allen and R. C. Dynes, Phys. Rev. B 12, 905 (1975).
[2]J. Muller, Rep. Prog. Phys. 43, 641 (1980).
[3]A. Junod, D. Bichsel, and J. Muller, Helv. Phys. Acta 52, 580 (1979).
[4]A. Junod and J. Muller, Solid State Commun. 36, 721 (1980).
[5]P. Spitzli, Phys. Kondens. Mater. 13, 22 (1971).
[6]R. G. Chambers, Proc. Phys. Soc. London 78, 941 (1961).
[7]A. Junod, Solid State Commun. 33, 55 (1980).
[8]A. Junod, J.-L. Staudenmann, J. Muller, and P. Spitzli, J. Low Temp. Phys. 5, 25 (1971).
[9]A. Junod, P. Bellon, R. Flükiger, F. Heiniger, and J. Muller, Phys. Kondens. Mater. 15, 133 (1972).
[10]A. Junod, Ph.D. thesis, Université de Genève, 1974 (unpublished).
[11]A. Junod, J. Muller, H. Rietschel, and E. Schneider, J. Phys. Chem. Solids 39, 317 (1978).
[12]E. Z. Kurmaev, V. P. Belash, R. Flükiger and A. Junod, Solid State Commun. 16, 1139 (1975).
[13]E. Bucher, F. Heiniger, and J. Muller, in *Proceedings of the Ninth International Conference on Low Temperature Physics, LT9, Columbus, Ohio, 1964,* edited by J. G. Daunt (Plenum, New York, 1965), Part A, p. 482.
[14]P. Garoche, P. Manuel, J. J. Veyssié, and P. Molinié, J. Low Temp. Phys. 30, 323 (1978).
[15]E. L. Wolf, J. Zasadzinski, G. B. Arnold, D. F. Moore, J. M. Rowell, and M. R. Beasley, Phys. Rev. B 22, 1214 (1980).
[16]G. S. Knapp, S. D. Bader, and Z. Fisk, Phys. Rev. B 13, 3783 (1976).
[17]B. M. Klein, L. L. Boyer, and D. A. Papaconstantopoulos, Phys. Rev. Lett. 42, 530 (1979).
[18]V. Z. Kresin and V. P. Parkhomenko, Fiz. Tverd. Tela

(Leningrad) 16, 3363 (1974) [Sov. Phys.—Solid State 16, 2180 (1975)].
[19]H. Padamsee, J. E. Neighbor, and C. A. Shiffman, J. Low Temp. Phys. 12, 387 (1973).
[20]S. J. Nettel and H. Thomas, Solid State Commun. 21, 683 (1977).
[21]B. T. Geilikman and V. Z. Kresin, Fiz. Tverd. Tela (Leningrad) 7, 3294 (1965) [Sov. Phys.—Solid State 7, 2659 (1966)].
[22]T. Jarlborg (unpublished); see also J. Phys. F 9, 283 (1979); T. Jarlborg, A. Junod, and M. Peter (unpublished).
[23]B. M. Klein, L. L Boyer, and D. A. Papaconstantopoulos, Phys. Rev. B 18, 6411 (1978).
[24]W. E. Pickett, K. M. Ho, and M. L. Cohen, Phys. Rev. B 19, 1734 (1979).
[25]A. T. van Kessel, Ph.D. thesis, University of Nijmegen, 1981 (unpublished); see also A. T. van Kessel, H. W. Myron, and F. M. Mueller, Phys. Rev. Lett. 41, 181 (1978).
[26]H. B. Radousky, T. Jarlborg, G. S. Knapp, and A. J. Freeman, Phys. Rev. B 26, 1208 (1982).
[27]G. R. Stewart and G. W. Webb, Solid State Commun. 33, 1015 (1980).
[28]G. R. Stewart, L. R. Newkirk, and F. A. Valencia, Solid State Commun. 26, 417 (1978).
[29]M. Pelizzone, Ph.D. thesis, Université de Genève, 1982 (unpublished).
[30]Ö. Rapp and C. Crafoord, Phys. Status Solidi B 64, 139 (1974).
[31]H. Rietschel and H. Winter, Phys. Rev. Lett. 43, 1256 (1979).
[32]H. Rietschel, H. Winter, and W. Reichart, Phys. Rev. B 22. 4284 (1980).
[33]J. J. Hopfield, Phys. Rev. 186, 443 (1969).
[34]W. L. McMillan, Phys. Rev. 167, 331 (1968).
[35]R. C. Dynes and C. M. Varma, J. Phys. F 6, L215 (1976).
[36]J. M. Daams, B. Mitrovic, and J. P. Carbotte, Phys. Rev. Lett. 46, 65 (1981).
[37]G. Riblet, Phys. Rev. B 3, 91 (1971).
[38]T. P. Orlando and M. R. Beasley, Phys. Rev. Lett. 46, 1598 (1981). A prefactor $\bar{I}$ is missing in Eq. (7); see Ref. 39.
[39]S. Doniach and S. Engelsberg, Phys. Rev. Lett. 17, 750 (1966).
[40]A. Junod, R. Flükiger, A. Treyvaud, and J. Muller, Solid State Commun. 19, 265 (1976). The two states of order were generated, respectively, by argon quenching from 1250°C and by slow cooling from 1250°C to 610°C.
[41]A. M. Clogston, A. C. Gossard, V. Jaccarino, and Y. Yafet, Phys. Rev. Lett. 9, 262 (1962).
[42]R. A. Hein, J. E. Cox, R. D. Blaugher, R. M. Waterstrat, and E. C. van Reuth, Physica (Utrecht) 55, 523 (1971).
[43]R. Flükiger, Ch. Susz, F. Heiniger, and J. Muller, J. Less-Common Met. 40, 103 (1975).